AWARD NUMBER: W81XWH-14-1-0183

TITLE: Endobronchial Photoacoustic Microscopy for Staging of Lung Cancer

PRINCIPAL INVESTIGATOR: Huabei Jiang

CONTRACTING ORGANIZATION: University of Florida
Gainsville, FL 32611

REPORT DATE: June 2015

TYPE OF REPORT: Annual report

PREPARED FOR: U.S. Army Medical Research and Materiel Command
Fort Detrick, Maryland 21702-5012

Principal Investigator/Program Director (Last, first, middle): Jiang, Huabei

1. REPORT DATE	**2. REPORT TYPE**	**3. DATES COVERED**
June 2015	Annual report	1 Jun 2014 - 31 May 2015

4. TITLE AND SUBTITLE
Endobronchial Photoacoustic Microscopy for Staging of Lung Cancer

5a. CONTRACT NUMBER

5b. GRANT NUMBER
W81xwh-14-1-0183

5c. PROGRAM ELEMENT NUMBER

6. AUTHOR(S)
Hua Huang, Huabei Jiang

E-Mail: hjiang@bme.ufl.edu

5d. PROJECT NUMBER

5e. TASK NUMBER

5f. WORK UNIT NUMBER

7. PERFORMING ORGANIZATION NAME(S) AND ADDRESS(ES)

Department of Biomedical Engineering,
University of Florida
JG56 BMS building
1275 center Dr.
Gainesville FL 32601

8. PERFORMING ORGANIZATION REPORT NUMBER

9. SPONSORING / MONITORING AGENCY NAME(S) AND ADDRESS(ES)

U.S. Army Medical Research and Materiel Command
Fort Detrick, Maryland 21702-5012

10. SPONSOR/MONITOR'S ACRONYM(S)

11. SPONSOR/MONITOR'S REPORT NUMBER(S)

12. DISTRIBUTION / AVAILABILITY STATEMENT

Approved for Public Release; Distribution Unlimited

13. SUPPLEMENTARY NOTES

14. ABSTRACT

This project is to propose an endoscopic photoacoustic imaging method for lung cancer staging. In order to obtain the image of the lymph node at different depths, the tunable liquid lens is demonstrated to evaluate the performance of tunable focusing. To achieve this goal, we work on this project based on the following aspects: 1. Characterization and optimization of the tunable acoustic lens. 2. Design and optimization of the housing of the probe. 3. Phantom experiments using the proposed probe. According to our current results, we have successfully demonstrated the prototype of the tunable endoscopic photoacoustic imaging probe and system. The lymph-node/tumor mimicking phantom and nanoparticle/dye for lymph node imaging have also been tested.

15. SUBJECT TERMS
Endoscopic photoacoustic imaging, lung cancer, tumor staging, tunable acoustic lens

16. SECURITY CLASSIFICATION OF:			**17. LIMITATION OF ABSTRACT**	**18. NUMBER OF PAGES**	**19a. NAME OF RESPONSIBLE PERSON**
a. REPORT	**b. ABSTRACT**	**c. THIS PAGE**			USAMRMC
Unclassified	Unclassified	Unclassified	Unclassified	16	**19b. TELEPHONE NUMBER** *(include area code)*

Standard Form 298 (Rev. 8-98)
Prescribed by ANSI Std. Z39.18

Table of Contents

Page

1. Introduction

Lung cancer diagnosis and staging are very important for clinical therapy and prognosis. Lung cancer has a high mortality rate of 85% after five years. To properly manage the treatment of patients, the staging of lung cancer needs to be accurately performed. Surgical resection is mostly preferred when the staging indicates an ipsilateral mediastinal lymph node metastases; whereas chemotherapy and radiotherapy could be more effective when contralateral metastases are confirmed by staging. Computed tomography (CT) or positron emission tomography (PET) can only yield presumptive clinical diagnosis for lung cancer, and invasive biopsy is necessary to be carried out for the confirmation of staging. Endobronchial ultrasound (EBUS)-guided transbronchial needle aspiration (TBNA) has been demonstrated as the most accurate and minimally invasive method for the biopsy of lymph node. However, the ultrasound-based imaging has an inherently low imaging contrast owning to the low acoustic impedance mismatch between different tissues. In order to make the image-guided needle aspiration less invasive and more efficient, imaging with higher contrast and resolution is required. Recently photoacoustic imaging has emerged to offer relatively high optical contrast and comparable penetration depth as ultrasound. Nevertheless, the challenge to integrate the photoacoustic imaging modality into endoscopy through trachea is the limited room for the implementation of scanning. We have identified the emerging tunable endoscopic photoacoustic tomography (EPAT) as a candidate for cancer staging imaging. EPAT uniquely combines the high contrast advantage of optical imaging and the high resolution advantage of ultrasound imaging in a single modality. We will use 3D printing technology to realize the probe miniaturization and tunable focal point that are necessary for endoscopic imaging at different depths. It has been proved that the size of lymph node is closely related to the staging of cancer, especially lung cancer. Therefore, imaging the lymph node at different depths may provide us with an excellent tool to identify the appropriate staging of lung cancer. This technology focused application has put together a truly multi-disciplinary research team involving researchers in imaging, molecular targeting, tunable focusing, cancer biology, and surgical oncology.

2. Keywords

Endoscopic photoacoustic imaging, tunable acoustic lens, lung cancer, tumor staging, lymph node

3. Accomplishments

What were the major goals of the project?

The proposed time line for project execution is presented in Table 1. We are pleased to report that we have made significant progress during the first year in developing the proposed tunable EPAT system. We first proposed an EPAT probe structure for lung cancer imaging. We also designed, fabricated, and characterized the EPAT probe using phantoms.

The following gives the originally proposed SOW:

1. Characterization and optimization of the tunable acoustic lens (months 1-3):

1a. Design the lens molds with different dimensions and print them using 3-D printer (month 1).

1b. Characterize the lenses with different numeric apertures and lensing liquids; Identify the relationships between the focal length and the infusion volume of the lensing liquid (month 2).

1c. Test the lenses in photoacoustic microscopy experiment and identify the optimum lens working for the specific transducer as well as the probe (month 3).

2. Design and optimization of the housing of the probe (months 4-5):

2a. Design the housing of the probe using sketchup with minimized and optimum dimensions and build it with 3-D printer (months 4-5).

2b. Assemble the transducer, acoustic lens, optical fiber, and mini-motor in the housing (months 5).

3. Phantom experiments using the proposed probe (months 6-8):

3a. Code the program for the data acquisition (month 6).

3b. Make the phantoms to mimic the trachea and lymph node structure (months 6-7).

3c. Carry out phantom experiments and image processing (months 7-8).

4. Assess the experimental results and make modifications (if needed) on the design (months 9-10):
4a. Analyze the experimental results and look into the technical issues (if any) (month 9).
4b. Make appropriate modifications (if needed) on the design to solve the technical issues (month 9).
4c. Repeat the experiments (if needed) to validate the modified design (month 9-10).

5. Produce a prototype of the design and write a final report on this project (months 11-12):
5a. Optimize the design and produce a prototype of the proposed probe (month 11).
5b. Write a final report on this project (month 12).

Table 1. Estimated project timeline.

Tasks\Months	1	2	3	4	5	6	7	8	9	10	11	12
1a												
1b												
1c												
2a												
2b												
3a												
3b												
3c												
4a												
4b												
4c												
5a												
5b												

What was accomplished under these goals?

In our task, we proposed to develop a complete tunable EPAT system. Here we report our effort in Year 1 in designing, fabricating, and testing these components.

3.1 Characterization and optimization of the tunable acoustic lens. (Task 1)

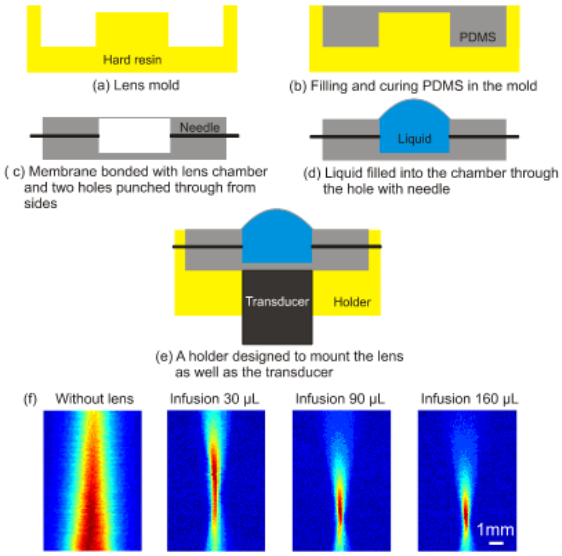

Figure1. Fabrication of the liquid acoustic lens (a)-(e), measurement of the tunable focal length (f)

In this work, we demonstrated a liquid acoustic converging lens with an adjustable focal length and apply it to photoacoustic microscopy. We have managed to fabricate a novel liquid acoustic lens, whose focal length can be dynamically tuned by the infusion volume of the liquid (Figure 1). The fabrication process of liquid acoustic lens is illustrated in figures 1 (a)-1(e). The mold can be printed by a 3-D printer (Objet Eden 260V). Liquid-phase PDMS is poured into the mold, and after 40 minutes baking at 80 degree Celsius the PDMS can be hardened. Then it is peeled off from the mold and bonded with another piece of PDMS membrane. The occupation of such a tunable acoustic lens for photoacoustic imaging could greatly save the room required by

scanning, since the axial scanning can be alternatively performed by tuning the acoustic focal length. Therefore, this may lead to a way to overcome the challenge to employ photoacoustic imaging method for endoscopy in trachea. The tunable function of this liquid acoustic lens is realized by pneumatically controlling the infusion volume of the liquid. Specifically, a syringe pump (KDS 210, KD Scientific) is used to accurately infuse or withdraw liquid into or from the lens chamber with a maximum pumping flow rate 474.8 ul/s when using B-D 5ml syringe. In this way, the lens interface, which is an elastic membrane, can be tuned with its curvature. Therefore, the focal length of this acoustic lens can be adjusted simply by changing the infusion volume of the liquid.

We choose silicone oil as the working liquid, which has a relative refractive index of 1.4 and density of 0.986 g/cm3. The higher refractive index (relative to water) as well as the convex shape of the lens will enable an ability of focusing acoustic beam. To characterize the focal length of this liquid acoustic lens, a transducer (30MHz, V213, Olympus) was used in its transmission mode for providing ultrasound pulses. The liquid acoustic lens was attached to the transducer head to focus the acoustic wave. A hydrophone (HGL-0200, ONDA) was used to scan laterally and axially while detecting the ultrasound pulses from the transducer. Figure 1(f) shows the comparison of pressure distributions between the transducers with and without the liquid acoustic lens. The arrow in the figure shows the propagation direction of the acoustic beam. The acoustic wave emitted from the transducer has a slightly focused wavefront (refer to the pressure mapping of transducer without the lens), which will eventually converge at the natural focus. When the transducer is working with the lens attached, the acoustic wave can be focused with variable focal length. Since the infusion volume of liquid determines the curvature of the lens, increasing the infusion volume by controlling the syringe pump can lead to a shortening of the focal length.

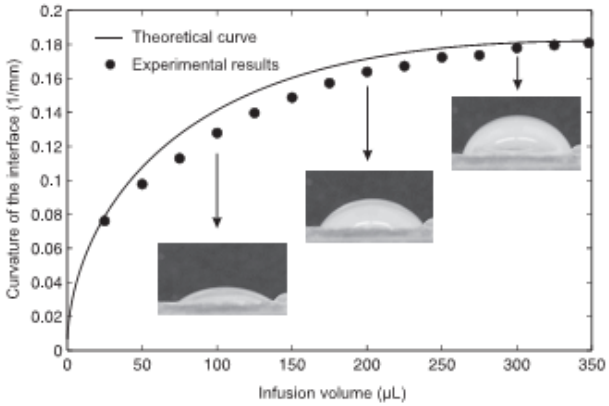

Figure 2. Curvature of the lens interface as a function of the infusion volume of liquid. The inset photographs illustrate the lens interface tuned by the infusion volume of the liquid.

The relationship between the curvature of the interface and the infusion volume of the liquid is characterized and shown in Figure 2. Assuming that the lens interface has aspherical shape and the liquid is incompressible, the infusion volume can mathematically determine the radius of the interface curvature (solid line in Figure 2) via

$$V = \pi h^2 (r - h/3), \tag{1}$$

where V represents the infusion volume of the liquid, and h and r denote the thickness of the lens and radius of the lens interface, respectively. The experimental results show a good agreement with the mathematical prediction. Setting this liquid acoustic lens on its focusing or diverging mode can be realized by purposely choosing the working liquid inside the lens chamber, which by principle is similar as manipulating optofluidic lens.

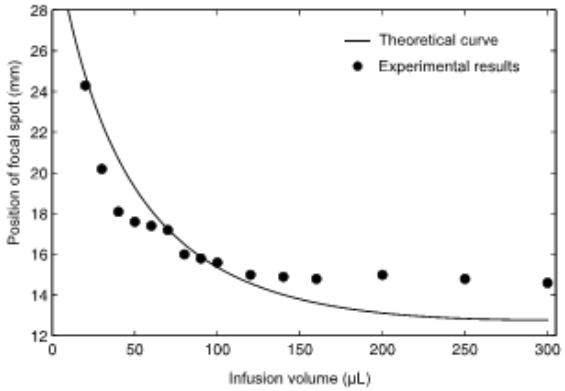

Figure 3. Focal length of the liquid acoustic lens as a function of the infusion volume of liquid.

Figure 3. shows the focal position as a function of the infusion volume of the liquid with both experimental results and theoretical analysis. The focal position can be mathematically calculated according to the conjugate relationship between image and object

$$\frac{1}{S_o}+\frac{1}{S_i}=\frac{1}{f}, \tag{2}$$

while considering the natural focus as the object So and focal position as the image Si. The position of the natural focus can be calculated by

$$S_o = D^2F/4c, \tag{3}$$

where D is the diameter of the transducer, F is the working frequency, and c is the velocity of sound. The theoretical focal length of the liquid acoustic lens can be derived as a function of infusion volume using Eq. (1)

$$f = (V/\pi h^2 + h/3)/(n-1), \tag{4}$$

where n is the acoustic refractive index. From Eqs. (2) to (4), the focal position can be obtained:

$$\frac{1}{S_i}=\frac{1}{(V/\pi h^2+h/3)/(n-1)}-\frac{4c}{D^2F}, \tag{5}$$

which is represented as the solid line in Figure 3. The results from the experiment show an agreement with the theoretical analysis. The purpose of this experiment is to give a validation that the liquid acoustic lens can effectively focus acoustic wave with variable focal length, and also provides a calibration of the relationship between the focal positions and the infusion volume for the later phantom experiment.

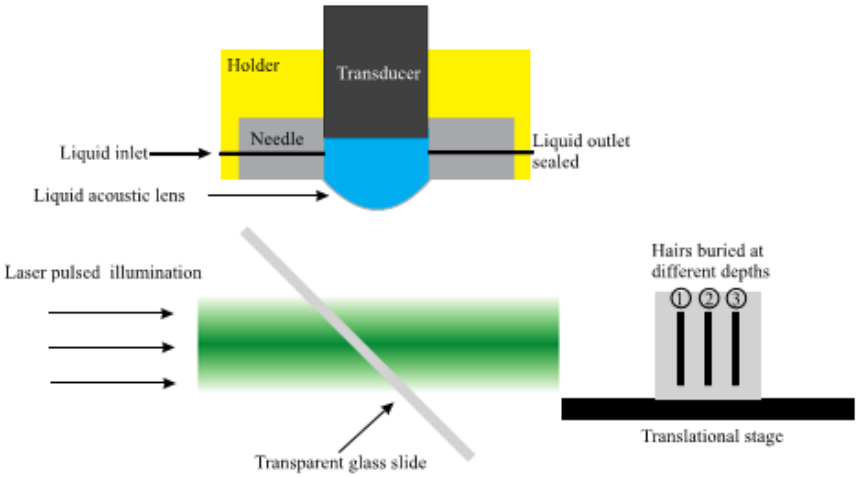

Figure 4. Schematic of the experimental setup. Test was carried out to validate the functionality of the adjustable liquid acoustic lens: (1) Three hairs were buried at different depths within the background phantom with 4mm distance between each hair.

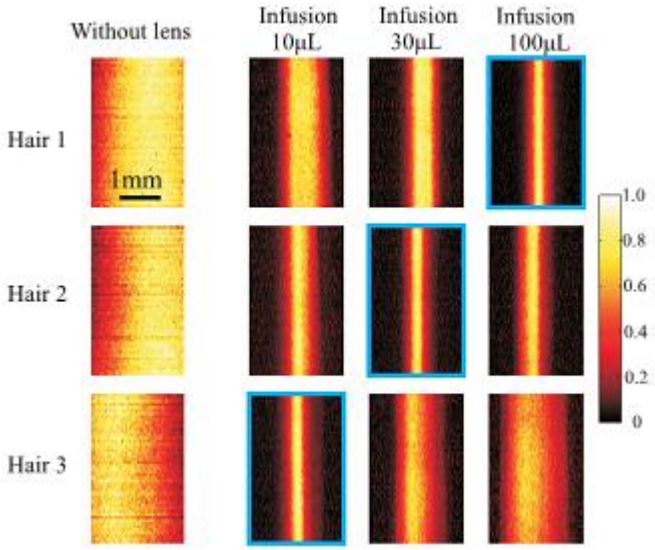

Figure 5. Images of hair by photoacoustic microscopy. Images of the three hairs in left column were captured by the 30MHz transducer without the liquid acoustic lens, and the other three column of images were captured with the lens under different conditions of infusion volumes.

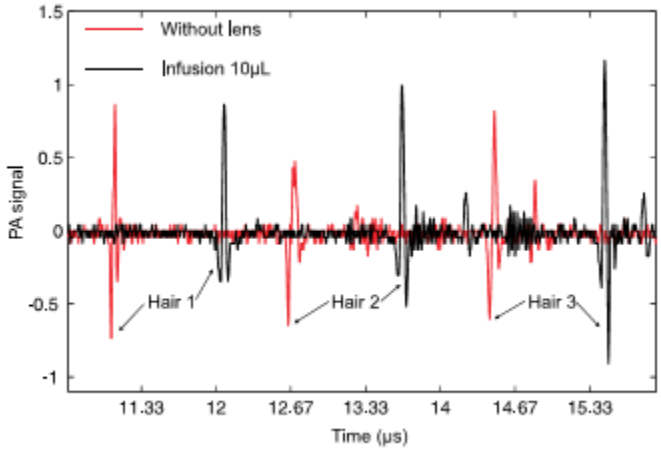

Figure 6. Comparison of photoacoustic signals from the three hairs. The red line denotes the PA signal collected without using liquid acoustic lens; the black line represents the PA signal collected using the lens with a liquid infusion volume of 10 ll.

The advantage of this liquid acoustic lens with an adjustable focal length lies in imaging objects at different depths without axial scanning of the detector. We designed and carried out tests to demonstrate this advantage using human hair as micro-scale targets (Figure 4). The targets were buried in a background with an absorption coefficient of ua= 0.007mm^{-1}and a reduced scattering coefficient us=0.1mm^{-1}. A 30MHz transducer (V213, Olympus) was used to collect the signal from the hair targets. The 30MHz transducer has outer diameter 11mm , and was equipped with corresponding lens whose apertures fit its outer diameter. The targets were illuminated and scanned by laser pulses with wavelength 532 nm and pulse duration 6 ns (NL 303HT, EKSPLA) coupled with a translational stage (Zaber Tech T-LSM200A).

Upon the energy deposition, an acoustic wave was generated from the local thermo-expansion and reflected by a glass slide to the ultrasound detector. The liquid acoustic lens was attached to the transducer and mounted on a hard-resin holder. The liquid was injected into the lens chamber through needle and tubing by a syringe pump (KDS 210, KD Scientific) with a flow rate of 1ul/s. During the data acquisition, the axial distance between the

targets and the transducer was fixed, and the translational stage provided a lateral scanning under each condition of infusion volume of the liquid.

For the hair imaging, three hairs were aligned in parallel and buried at different depths within the background phantom with 2.4mm distance between each other. The photoacoustic signal was first collected without using the liquid acoustic lens and processed with maximum amplitude projection (MAP) method. The images of the hairs (left column in Figure 5) show a broadened profile regarding the thickness of the hair. This lack of image fidelity is owing to the finite size of the effective diameter of the transducer. Considering the transducer has an effective diameter of several millimeters, the hairs were imaged to have approximately the same size regarding the thickness. After the transducer was equipped with the liquid acoustic lens, the PAM system managed to obtain sharper images of the hairs (with blue outlines in Figure 5) when the focus of the lens was axially adjusted to coincide with the position of the hair. During the test, the focal length was continuously shortened by increasing the infusion volume of liquid. Thus, hair 3, which was the farthest from the transducer, was first focused and imaged under a condition of low infusion volume of 10 ul. With the infusion volume going higher and focal length getting shorter, hair 2 and hair 1 came to their focus afterwards and were sharply imaged under the infusion conditions of 30 ul and 100ul, respectively.

We also looked into the comparison of photoacoustic signals between using and without the liquid acoustic lens, which is shown in Figure 6. The red line denotes the PA signal collected without using the liquid acoustic lens; the black line represents the PA signal collected using the lens with a liquid infusion volume of 10 ul. The collected PA signals from hair 2 and 3 when using the lens are stronger than those collected without the lens, while the difference of the PA signals of hair 1 goes to the opposite way. When employing the liquid acoustic lens with a 10 ul infusion volume, the focus was approximately located near the regions of hair 2 and 3, so a larger volume of the spherically radiating PA signals can be covered and collected by the transducer. On the other hand, the bare transducer can only take in the PA waves with Poynting vectors that fit the limited directivity of the transducer. With regard to hair 1, its position was relatively farther from the focus of the lens, so the spherical PA waves can hardly be converged to enter the transducer. Meanwhile, part of the PA signal could be reflected by the lens membrane, so the overall detected signal from hair 1 when using the lens is less than that using the bare transducer.

3.2 Design and optimization of the housing of the probe. (Task 2)

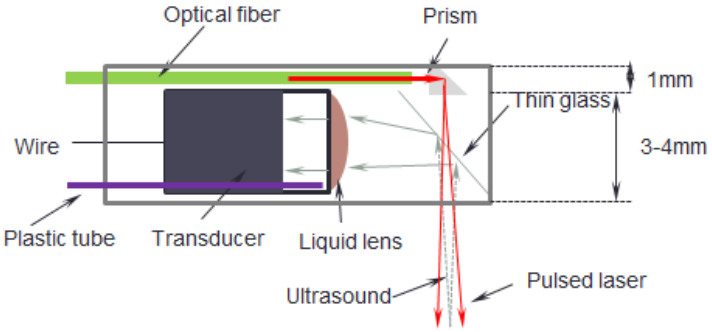

(a)

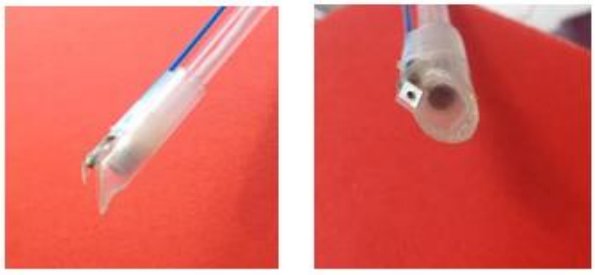

(b)

Figure 7. (a) Structure of the endoscopic PAT probe, (b) Fabricated endoscopic PAT probe

Figure 7 (a) illustrates the schematic of the probe for endobronchial photoacoustic microscopy based on the tunable acoustic lens, (b) shows the side view and front view of the fabricated endoscopic probe for PA imaging. A 10MHz transducer (3mm diameter, Olympus) is mounted along the central axis of the probe. The liquid acoustic lens is attached to transducer with ultrasound gel in between. The liquid, silicone oil with an acoustic refractive index 1.55, can be pumped into the lens chamber through the tunnel buried in the housing of the probe. The curvature of the lens interface can be controlled in a pneumatic way by an external syringe pump (KDS 210, KD Scientific). An optical fiber is employed to deliver the laser pulse through the window, which is located at the side of the probe. The window is sealed with a polydimethylsiloxane (PDMS) membrane, which is bio-compatible and can make a seamless contact with the trachea wall. When the tissues receive the pulsed electromagnetic energy, thermal vibration can be initiated and detected by the transducer. Indocyanine green can be used by exogenous injection to introduce better image contrast of the lymph nodes. A transparent glass slide is mounted to reflect the acoustic wave into transducer. By spinning the probe using the motor and tuning the focal length of the liquid acoustic lens, the transducer can cover a detection area. Owing to the tunable lens, the scanning process can be exempted from translating the transducer. And this makes the photoacoustic microscopy feasible for the endobronchial application.

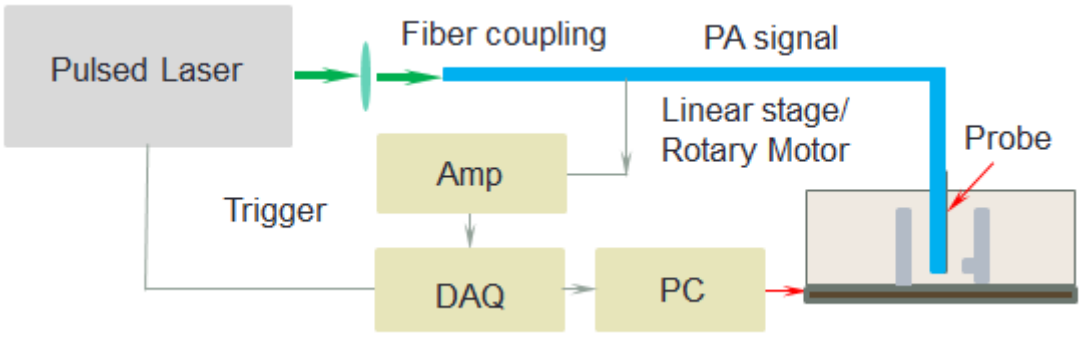

Figure 8. The whole EPAT imaging system

Figure 8 is the EPAT system for imaging. This imaging system consists of illumination part, acoustic detection part, rotation part, and data acquiring unit. The pulsed laser is used to illuminate the target to generate the photoacoustic (PA) signals. The plused laser from a Ti: Sapphire laser tunable (690 to 950 nm) is delivered to the target through the optical fiber, which is connected to the probe. The generated acoustic signals are collected by the transducer from 360 degree while the rotator is moving. The electrical signals of acoustic transducer are received by the data acquiring unit mounted on the computer with synchronic controlling. The PC is used to control the whole system for imaging and process the data for post processing.

3.3 Phantom experiments using the proposed probe. (Task 3)

The endoscopic probe has been demonstrated for evaluating the planar imaging ability firstly. The diameter of the fabricated probe is about 6mm which can be used for imaging the lymph node of human lung cancer. The phantom experiment is conducted by using three hairs at different depths illustrated in figure 9. The hairs are separated by 5mm and 5mm along axial and lateral directions, respectively. The wavelength used to generate the acoustic signals is 532nm. The PA images shown in Figure 9 are obtained under three conditions: no focusing, out of focusing, and focal point at target 1, 2, and 3. The intensity and the diameter of the targets are analyzed quantitatively in figure 9 for the top, mid and bottom hairs. Based on the results, the focal point can be adjusted by injecting the silicon oil from 0 to 50 ul into the tube connected with the acoustic lens. The PA intensity can be increased when the focal point of the acoustic lens is focused on the target. The lateral resolution can be improved to about 300-400um by the focusing at the target, while the axial resolution about 200-300 um is decided by the frequency of the transducers. When the target is off the focal point or not focused, the intensity and lateral resolution are lower compared to the focused point. When the target is located more than 15mm, the signal is getting worse.

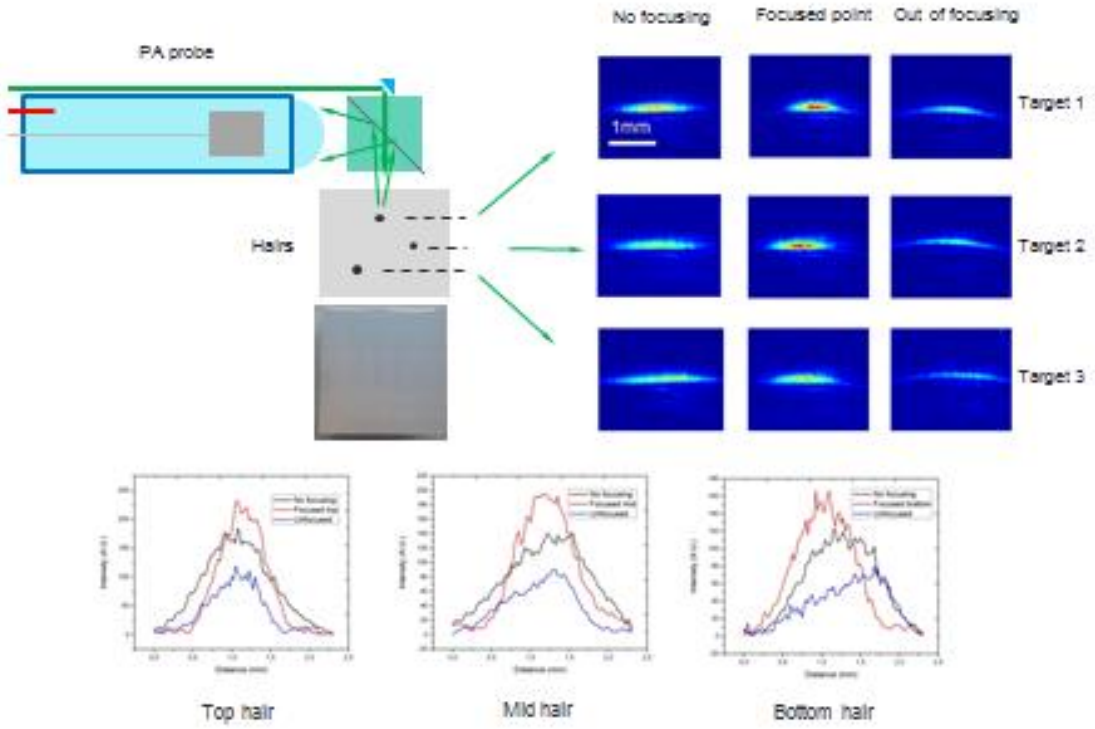

Figure 9. The PA imaging of hair phantom experiments using EPAT probe

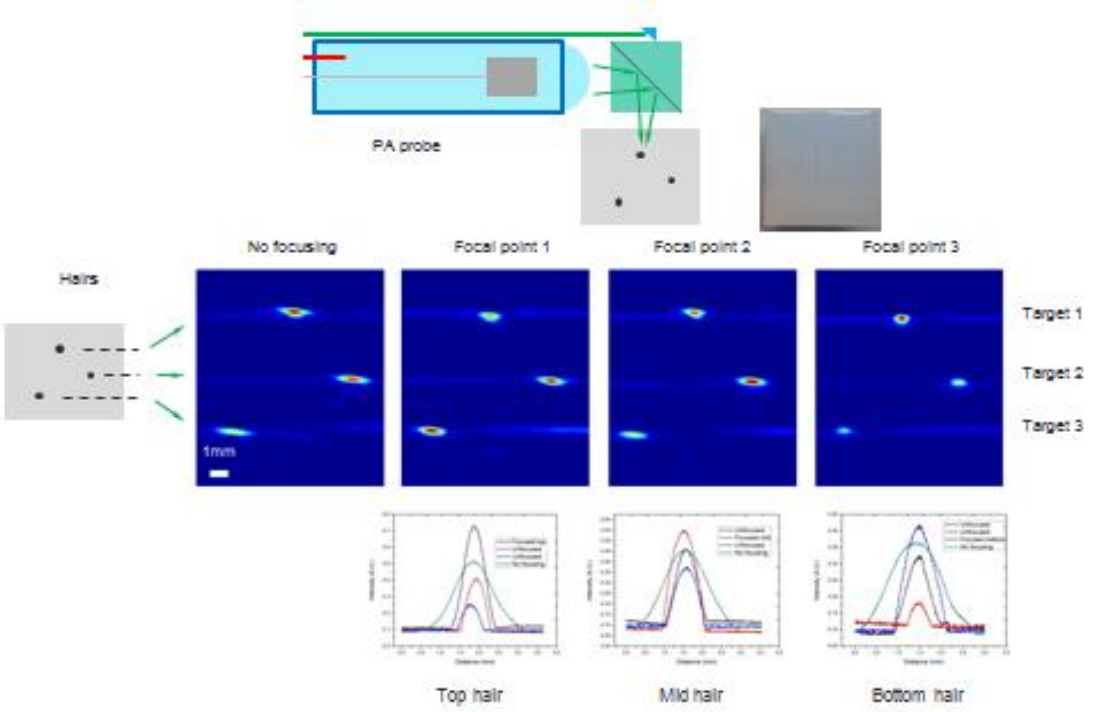

Figure 10. The ultrasound image of hair phantom experiments using EPAT probe

The ultrasound images of the hair phantom are also obtained to evaluate the tunable focusing abilities, shown in figure 10. The setup of this ultrasound imaging method uses the same structure of probe but without the illumination of the pulsed laser. The focal point is adjusted by injecting the silicon oil into lens chamber. The ultrasound images in figure 10 are reconstructed by using the reflected ultrasound signals. Intensity and the diameter of the targets are analyzed to evaluate the image quality. According to the result in figure 10, the focal point has the best lateral resolution and strongest contrast. The EPAT probe can successfully image the target at different depths within 15mm. The conclusion is similar to the PA results shown in figure 9. However, the

ultrasound image has better signal to noise ratio due to the high penetration of the ultrasound signals as source. Base on the 2D image, we explored the 3D imaging using the same probe by adding an extra scanning in Z direction. The 3D reconstructed images are shown in Figure 11. The top hair target is imaged under no focusing and focused conditions. The top view and side view of the top hair show that the target has the best intensity and resolution when it is well focused compared to the image with no focusing.

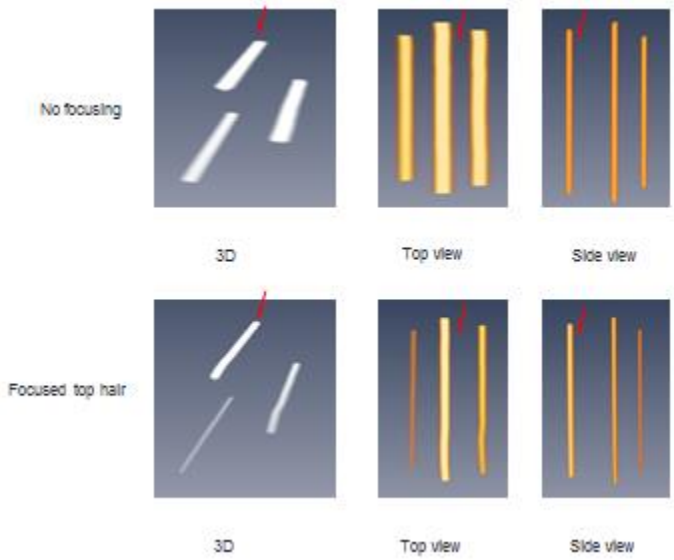

Figure 11. The 3D image if reconstructed hair phantom

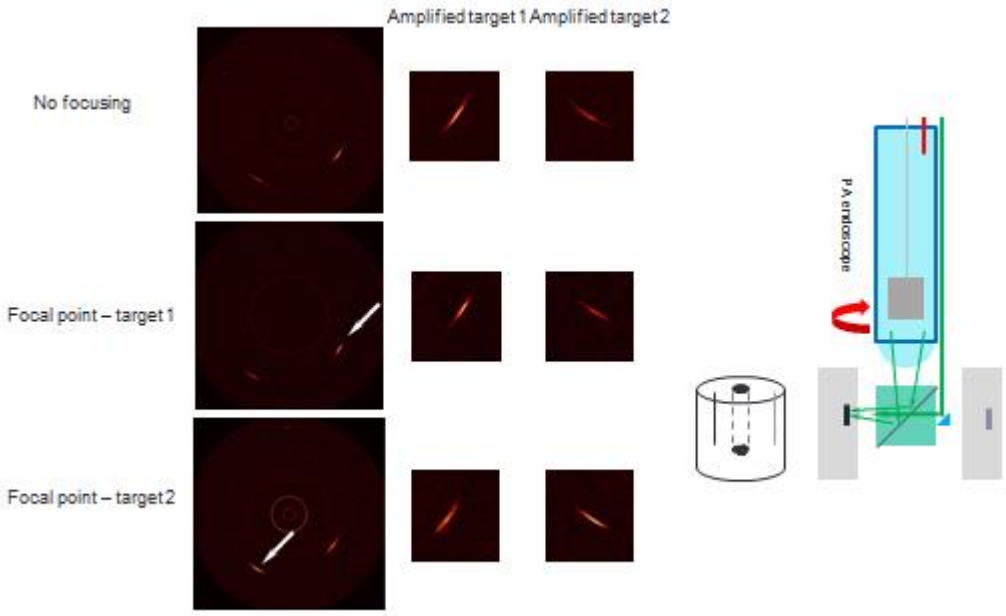

Figure 12. The endoscopic PA image of copper wire phantom using the EPAT probe

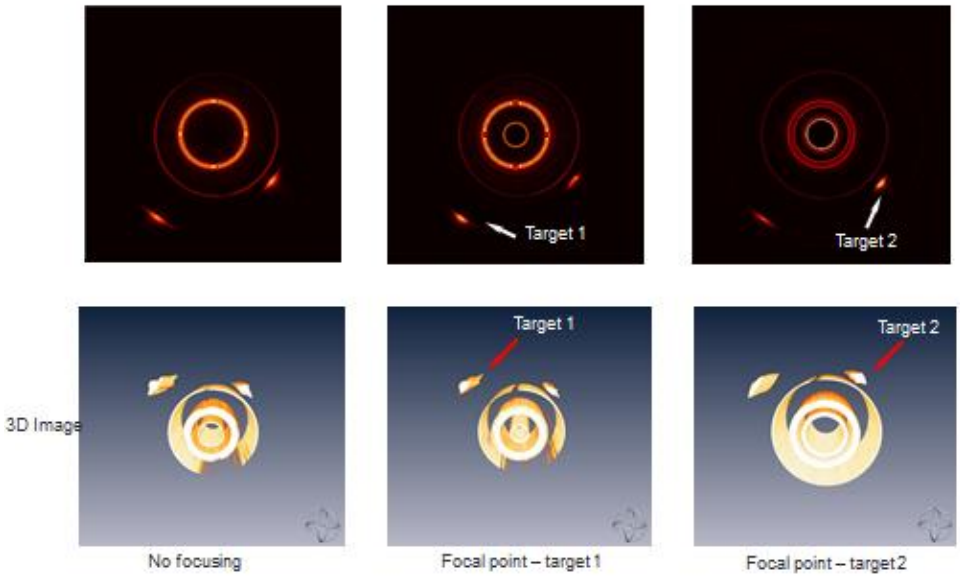

Figure 13. The endoscopic US image of copper wire phantom using the EPAT probe

The endoscopic imaging performance of the EPAT probe is evaluated by rotating the probe to obtain the image from 360 degree. This imaging method is used to test the endoscopic imaging ability for lung cancer. Two targets of copper wires with diameter of 0.1mm are imaged using this EPAT probe shown in figure 12. The right side shows the structure of the setup and phantom. The left side shows the image results of the two targets with and without focusing. When the focal point is moved to target 1, the lateral resolution is improved and the intensity is also increased compared to the no focusing condition. The same conclusion is drawn based on the target 2, but the deeper depth decreased the image quality of target 2. Figure 13 is the result of endoscopic ultrasound image of copper wires using the same probe and phantom. The probe also shows the ability to image the targets for ultrasound reconstruction by adjusting the focal point at different depths. 3D images are reconstructed in figure 13 (lower row) to show the image ability of this probe for non-focusing and focusing. The target 1 and 2 can be imaged sharply when the focal point is focused at the right depth. So far, we have finished the evaluating the probe using standard phantoms. This integrated tunable acoustic probe has the ability to image targets as small as 100um at the depth of about 1cm.

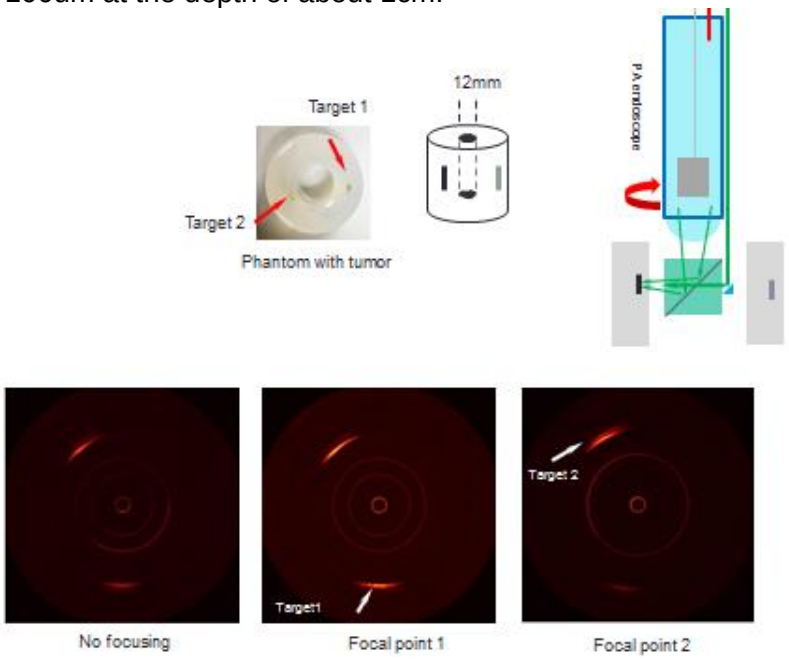

Figure 14. The endoscopic PA image of tumor phantom using the EPAT probe

Based on the phantom experiments using hairs and copper wires, we extended the experiments to using the phantom mimicking solid tumor to evaluate the imaging performance of the endoscopic probe for a real target. In figure 14, two tumor targets are embedded inside the phantom with the separation of 3mm along the axial direction. The size of the tumor is about 2*5*5mm for thickness, width and length, respectively. The setup of the endoscopic imaging is the same as shown above. During the test, the infusion volume of acoustic lens was increased and under each condition of infusion volume, circular scanning was performed for the data acquisition. When the infusion volume went up to 5 ul, tumor 1, which was further away from the transducer, came into focus, while tumor 2 was out of focus to have a blurred image. As the infusion volume was increased to 50 ul leading to a shorter focal length, tumor 2, which was closer to the transducer, came into focus and was shapely imaged. Using this liquid acoustic lens, two targets with an axial distance of 3-5mm can be imaged without the implementation of axial scanning but alternatively by adjusting the focal length of the acoustic lens.

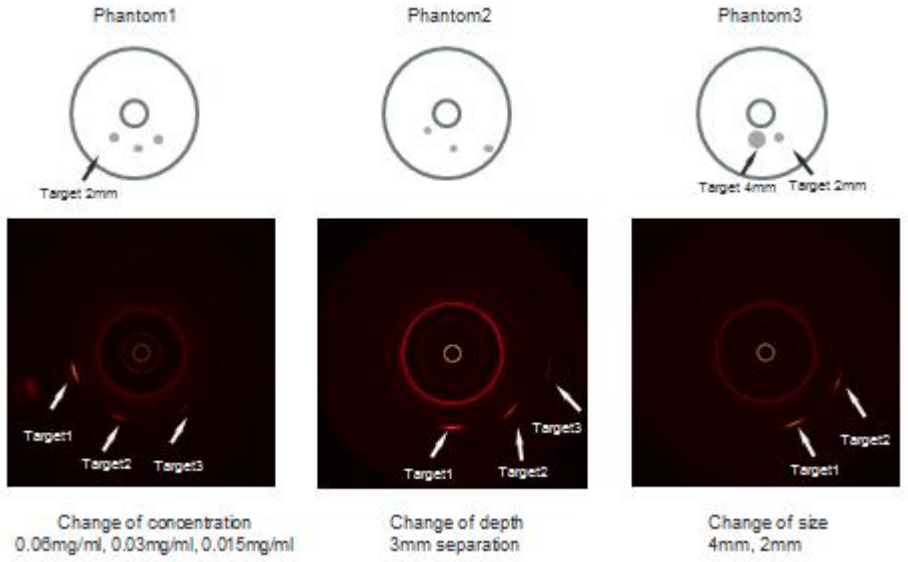

Figure 15. The endoscopic PA image of nanoparticle phantom using the EPAT probe

In the real situation of lymph node, the tissue does not include optical absorber which is important for PA imaging. To image the lymph node, the dye or absorber is necessary to generate the acoustic signals for PA signals. Three kinds of lymph node mimic phantoms are tested with the graphene as the optical absorber. In figure 15, phantom 1 has three targets with different concentrations of graphene solution: 0.06mg/ml, 0.03mg/ml and 0.015mg/ml. By changing the concentration, we can find the best concentration for PA imaging. The results show that the 0.06mg/ml can provide clear image quality for PA imaging. The phantom2 shown in figure 15 includes three targets at different depths (3mm separation) with same concentration of graphene 0.06mg/ml. The results indicated that the deeper depth decreases the intensity of the signal and image quality even the concentrations of the absorber are the same. The phantoms3 is designed to evaluate the ability of this imaging method to differentiate the size of the targets. Two targets with different size: 4mm and 2mm are included in the phantom. According to the reconstructed images, it is easy to tell the different size of the target by measuring the lateral length of the reconstructed targets.

3.4 Assess the experimental results and make modifications (if needed) on the design. (Task 4)

We have successfully demonstrated the endoscopic imaging of PAT probe for tunable focusing. The results are based on the delay-sum reconstruction. We still working on this project to improve the system in the following aspects:

1. Minimize the probe size to 4-5mm to so that it can be applied to the human lung cancer diagnosis in future.
2. Optimize the light delivery part so that maximized light delivery can be ensured for improved PA imaging..
3. Improve the image reconstruction method to reduce the false lateral length introduced by the reconstruction.

3.5 Produce a prototype of the design and write a final report on this project. (Task 5)

We are working on minimizing the probe and will finish all the phantom experiments that mimic real lymph node of human. The final report will be written upon the end of this project.

What opportunities for training and professional development has the project provided?
Nothing to Report

How were the results disseminated to communities of interest?
Nothing to Report

What do you plan to do during the next reporting period to accomplish the goals?

We have made satisfactory progress on hardware design and fabrication for the EPAT system, and completed aim as proposed for Year 1 of this project. We even exceed the work statement of Year 1 with some initial phantom studies of the fabricated devices. Given the successful progress in Year 1, we will be able to fulfill the work statement for Year 2. Specifically, we will perform considerable phantom experiments to test and evaluate the minimized EPAT system. We will also follow with evaluation of the efficacy of EPAT imaging to quantify the impact of proposed system on tumor staging. One manuscript is already under preparation, and we plan to have 2-3 journal papers based on the studies in Years 1 and 2. We also plan to submit numerous abstracts for conference presentation.

4. Impact

What was the impact on the development of the principal discipline(s) of the project?
Currently lung cancer is the leading cause of death in the United States. An accurate staging of metastasis status determines the optimum management of treatment to patients. Medical imaging diagnosis alone is not sufficient and only yields a suspicion of metastasis. Invasive biopsy has to be carried out to confirm the staging. The proposed research of developing a novel endobronchial photoacoustic microscopy will lead to a less invasive and more efficient method to guide the fine needle aspiration of lymph node. It will also help doctor to evaluate the tumor staging to improve the diagnosis and the consequent therapy.

What was the impact on other disciplines?
Nothing to Report

What was the impact on technology transfer?
Nothing to Report

What was the impact on society beyond science and technology?
Nothing to Report

5. Changes/Problems

Changes in approach and reasons for change
Nothing to Report

Actual or anticipated problems or delays and actions or plans to resolve them
Nothing to Report

Changes that had a significant impact on expenditures
Nothing to Report

Significant changes in use or care of human subjects, vertebrate animals, biohazards, and/or select agents
Nothing to Report

Significant changes in use or care of human subjects
Nothing to Report

Significant changes in use or care of vertebrate animals.
Nothing to Report

Significant changes in use of biohazards and/or select agents
Nothing to Report

6. Products

Publications, conference papers, and presentations
Nothing to Report

Website(s) or other Internet site(s)
Nothing to Report

Technologies or techniques
Nothing to Report

Inventions, patent applications, and/or licenses
Nothing to Report

Other Products
Nothing to Report

7. Participants & Other Collaborating Organizations

What individuals have worked on the project?

Name:	*Hua Huang, Chaolong Song*
Project Role:	*Graduate Student, Postdoc*
Researcher Identifier (e.g. ORCID ID):	
Nearest person month worked:	7
Contribution to Project:	*Mr. Huang and Song have performed work in the area of tunable endoscopic PA imaging.*
Funding Support:	

Has there been a change in the active other support of the PD/PI(s) or senior/key personnel since the last reporting period?

None.

What other organizations were involved as partners?
Nothing to Report

8. Special Reporting Requirements

Nothing to Report

9. Appendices

Nothing to Report